

# Animation of Electric and Magnetic Field Lines

James Parsloe

*St. John's College,  
University of Cambridge*

Project Supervisor: Prof. Stephen Gull

(Dated: May 10, 2015)

An article usually includes an abstract, a concise summary of the work covered at length in the main body of the article.

## CONTENTS

I. Introduction	1
A. What is a field line?	1
B. MATLAB	1
C. Maxwell's Equations	1
II. Magnetic field lines	2
A. Azimuthally symmetric field lines	2
B. Rotating geometries in external fields	2
1. Rotating axisymmetric conductors in axial fields	3
2. Rotating Cylinder in a Transverse Field	3
3. Rotating Sphere in a Transverse Field	3
III. Electric field lines	3
A. Method of images	8
1. Point charges and planes	8
2. The point charge and conducting sphere	8
B. The uniformly charged disc	12
1. Point charge outside a dielectric sphere	12
C. Complex potentials	12
D. Electric dipole radiation	13
E. Relativistic field lines	14
1. Uniformly accelerated charge	14
2. Uniform circular motion	14
3. Harmonically oscillating charge	14
IV. Numerical work	14
A. Finite difference methods	15
B. Solving the field line equations	15
1. Runge-Kutta methods	15
A. First Appendix	15
References	23

## I. INTRODUCTION

The concept of the 'field' and in turn field lines has its origins with Faraday and Maxwell (Maxwell, 1864, 1861, 1873) Field lines are an extremely good way of visualising vector fields.

### A. What is a field line?

A field line is a curve which is tangent at all points to the underlying vector field  $B$ . Mathematically we can

write this as:

$$\frac{d\mathbf{x}_S}{ds} \times \mathbf{B}(\mathbf{x}_S) = 0 \quad (1)$$

where  $\mathbf{x}_S(s)$  is the parametric representation of a single field line. From this definition it then follows that:

$$\frac{dx_S}{B_x} = \frac{dy_S}{B_y} = \frac{dz_S}{B_z} \quad (2)$$

where the components of the vector field are  $\mathbf{B} = (B_x, B_y, B_z)$  and those of the streamline are  $\mathbf{x}_S = (x_S, y_S, z_S)$ . In general in order to find the field lines we need to solve these differential equations. However, in some cases it is indeed possible to circumvent these steps.

The problem of visualising streamlines is largely then two-fold: firstly, we need to generate the underlying vector field and then we need to solve the differential equations that describe the field line and plot them. Although, as stated previously, many cases can be resolved without the need to follow this algorithmic approach.

## B. MATLAB

MATLAB is a high-level technical computing language with many built in functions, as well as visualisation tools. This makes it as quick and easy way to create field lines.

## C. Maxwell's Equations

Of course, the starting point for the study of electric and magnetic field lines begins with Maxwell's equations:

$$\nabla \cdot \mathbf{D} = \rho \quad (3)$$

$$\nabla \cdot \mathbf{B} = 0 \quad (4)$$

$$\nabla \times \mathbf{E} = -\frac{\partial \mathbf{B}}{\partial t} \quad (5)$$

$$\nabla \times \mathbf{H} = \mathbf{J} + \frac{\partial \mathbf{D}}{\partial t}, \quad (6)$$

where the auxiliary fields  $\mathbf{D}$  and  $\mathbf{H}$  have the standard definitions  $\mathbf{D} = \epsilon_o \mathbf{E} + \mathbf{P}$  and  $\mathbf{H} = \mathbf{B}/\mu_o - \mathbf{M}$ .

## II. MAGNETIC FIELD LINES

### A. Azimuthally symmetric field lines

In the case of azimuthally symmetric geometries the calculation of the magnetic field lines can be considerably simplified if a suitable vector potential  $\mathbf{A}$  can be found that satisfies  $\mathbf{B} = \nabla \times \mathbf{A}$ . The field lines are then simply contours of  $\rho A_\phi$  where  $A_\phi$  is the azimuthal component of the vector potential and  $\rho$  is the radial distance in cylindrical coordinates. This can easily be shown with the use of the expression for the curl of axially symmetric  $\mathbf{A}$  in cylindrical coordinates:

$$\mathbf{B} = \frac{1}{\rho} \frac{\partial(\rho A_\phi)}{\partial \rho} \hat{\mathbf{z}} - \frac{\partial A_\phi}{\partial z} \hat{\mathbf{r}}. \quad (7)$$

It is then clear that we can form the field line equation in the  $\rho - z$  plane as:

$$\frac{dz}{d\rho} = -\frac{\partial_\rho(\rho A_\phi)}{\partial_z(\rho A_\phi)} \quad (8)$$

which can then be easily integrated to show that field lines satisfy the condition  $\rho A_\phi$  is constant. This approach circumvents the standard procedure of calculating the field and then solving the differential equations, however, it is a quirk of the vector potential formulation in azimuthally symmetric geometries.

The simplest implementation of this feature is with the circular current loop whose vector potential lies solely in the azimuthal direction from symmetry considerations. The form of the vector potential can then be expressed in terms of the complete elliptic integrals  $K$  and  $E$ : (Jackson, 1998)

$$A_\phi = \frac{\mu_o}{4\pi} \frac{4Ia}{\sqrt{a^2 + r^2 + 2a\rho}} \left[ \frac{(2 - k^2) K(k) - 2E(k)}{k^2} \right] \quad (9)$$

where

$$k^2 = \frac{4a\rho}{a^2 + r^2 + 2a\rho} \quad (10)$$

and  $r$  and  $\rho$  are the usual spherical and cylindrical coordinates respectively. Fig. (1) then shows the field lines as contours of  $\rho A_\phi$  spaced at aesthetically pleasing values.

It is then a simple procedure to generalise the current loop to the case of a solenoid through a convolution of the current ring field and a vertical array. The  $\mathbf{B}$  field lines of this solenoid are the same as those for a bar magnet as shown in Fig. (2).

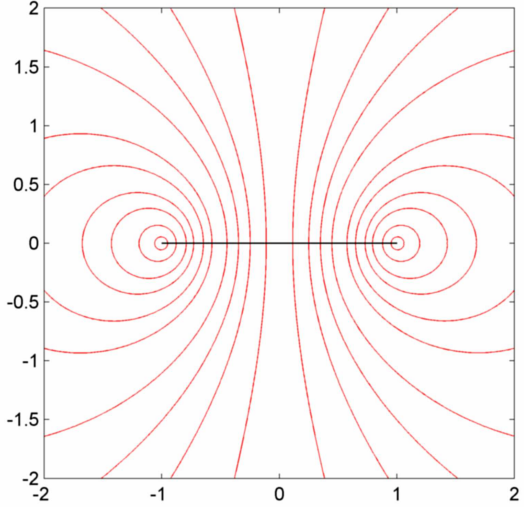


FIG. 1 Magnetic field lines from a circular current loop

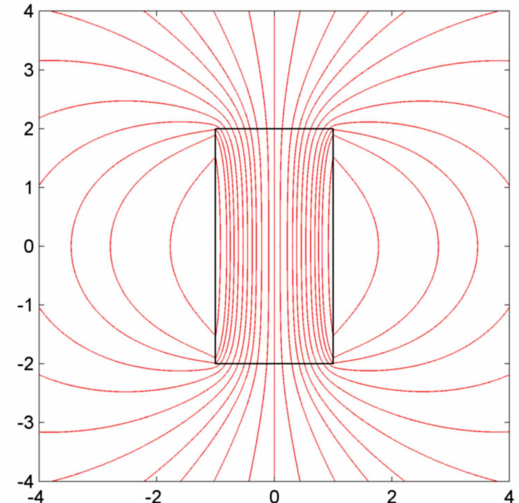


FIG. 2 Magnetic  $\mathbf{B}$  field lines for a bar magnet

### B. Rotating geometries in external fields

Rotating geometries are a natural generalisation of the static cases we have considered previously. They are also seen a lot less frequently in the literature due to the often complicated expressions and derivations.

The solutions are dependent on a magnetic Reynolds number  $R_m$  which is entirely analogous to the fluid Reynolds number.

In the following cases the fields for the rotating cylinder and rotating sphere in transverse constant magnetic fields are considered. The key physical point behind the field

line diagrams is that internal eddy current are induced which tend to oppose the external field are induced. The larger the magnetic Reynolds number the more the external field is expelled from the conductor.

The derivation of the fields for the rotating cylinder and rotating sphere in transverse fields begins in the same way. Of course we begin with Maxwell's equations and supplement them with:

$$\mathbf{J} = \sigma(\mathbf{E} + \mathbf{v} \times \mathbf{B}). \quad (11)$$

Inserting this expression into Eq. (6) and neglecting the displacement current term, which is valid in quasi magnetostatic situation, we get:

$$\nabla \times \mathbf{B} = \mu\sigma(\mathbf{E} + \mathbf{v} \times \mathbf{B}). \quad (12)$$

Taking the curl of both sides of Eq. (12) and using Eq. (5) we arrive at:

$$\nabla \times (\nabla \times \mathbf{B}) = \mu\sigma(\nabla \times \mathbf{E} + \nabla \times (\mathbf{v} \times \mathbf{B})) \quad (13)$$

$$= \mu\sigma(-\frac{\partial \mathbf{B}}{\partial t} + \nabla \times (\mathbf{v} \times \mathbf{B})). \quad (14)$$

Then using the standard vector identity  $\nabla \times (\nabla \times \mathbf{B}) = \nabla(\nabla \cdot \mathbf{B}) - \nabla^2 \mathbf{B}$  we arrive at what is known as Bullard's equation:

$$-\nabla^2 \mathbf{B}/\mu\sigma = -\frac{\partial \mathbf{B}}{\partial t} + \nabla \times (\mathbf{v} \times \mathbf{B}). \quad (15)$$

This is valid for the interior of the conductor where free currents flow and we shall from now on denote the interior solution as  $\mathbf{B}^{in}$ . Outside of the conductor, no free current flows and hence we can derive the magnetic field from a suitable scalar potential such that  $\mathbf{B}^{ex} = -\mu_0 \nabla \psi$  with the condition  $\nabla^2 \psi = 0$ .

These are entirely general vector relations. However, the approach for the rotating cylinder and sphere must diverge now to take account of the specific forms of the vector Laplacian in cylindrical and spherical coordinates, as well as the fitting of boundary conditions.

## 1. Rotating axisymmetric conductors in axial fields

An axisymmetric conductor rotating in an applied axial magnetic field does not affect the applied field. If the external field  $\mathbf{B}^{ex}$  is symmetric about the axis of rotation then the total magnetic field  $\mathbf{B} = \mathbf{B}^{ex} + \mathbf{B}^{ind}$  is also axisymmetric. We can see this by taking the curl of Eq. (11) and noticing that  $\nabla \times \mathbf{E} = -\partial \mathbf{B}/\partial t = 0$  in the steady state. We then write

$$\nabla \times \mathbf{J} = \sigma[\Omega \rho \hat{\phi} \times (B_\rho \hat{\rho} + B_\phi \hat{\phi} + B_z \hat{z})] \quad (16)$$

$$= \sigma \Omega \nabla \times (-\rho B_\rho \hat{z} + \rho B_z \hat{\rho}) \quad (17)$$

$$= \sigma \Omega [\partial_\rho(\rho B_\rho) + \partial_z(\rho B_z)] \hat{\phi} \quad (18)$$

$$= \sigma \Omega \rho (\nabla \cdot \mathbf{B}) \hat{\phi} \equiv 0. \quad (19)$$

That is, the curl of the current density vanishes within the conductor. Stoke's theorem allows us to write

$$\oint_C \mathbf{J} \cdot d\mathbf{l} = \int_A (\nabla \times \mathbf{J}) \cdot d\mathbf{A} = 0 \quad (20)$$

Since  $C$  is an arbitrary closed contour within the conductor we can conclude that  $\mathbf{J} \equiv 0$  within the conductor and hence there can be no induced magnetic field. We then see that from Eq. (11),  $\mathbf{E} = -(\mathbf{v} \times \mathbf{B})$ . That is, the induced electric charge distribution perfectly cancels the  $\mathbf{v} \times \mathbf{B}$  field.

We are hence entirely capable of deriving the forms of the electric field that is generated by the external magnetic field. Conductors usually carry a surface charge.

It can be shown that the free charge density is given by  $Q_f = -\epsilon_0 \nabla \cdot (\mathbf{v} \times \mathbf{B})$ . For an axisymmetric conducting rigid body that is rotated about its symmetry axis at  $\Omega$  in a uniform axial field  $\mathbf{B} = B \hat{z}$  we find that  $\nabla \cdot (\mathbf{v} \times \mathbf{B}) = 2\Omega B$  and hence the induced free charge is  $-2\epsilon_0 \Omega B$ . For a rotating sphere using Gauss' law we hence see that a uniform radial field  $\mathbf{E} = -(2/3)\Omega B r \hat{r}$  is generated from this volume charge. A surface charge is then generated to compensate for this. The surface charge density can be shown to be  $S_f = \epsilon_0 \Omega B ((5/2) \sin^2 \theta - 1)$

## 2. Rotating Cylinder in a Transverse Field

The velocity in a cylinder uniformly rotating about the  $z$  axis at any point is given by  $\mathbf{v} = \Omega \rho \hat{\phi}$ . Hence for a field  $\mathbf{B} = B_\rho \hat{\rho} + B_\phi \hat{\phi} + B_z \hat{z}$  the  $\mathbf{v} \times \mathbf{B}$  term evaluates to  $B_z \rho \Omega \hat{\rho} - B_\rho \rho \Omega \hat{z}$  and taking the curl of this in cylindrical coordinates we arrive at

$$\begin{aligned} \nabla \times (B_z \rho \Omega \hat{\rho} - B_\rho \rho \Omega \hat{z}) &= \frac{1}{\rho} (\partial_\phi(-B_\rho \Omega \rho)) \hat{\rho} + \\ &(\partial_z(B_z \Omega \rho) - \partial_\rho(-B_\rho \rho \Omega)) \hat{\phi} + \frac{1}{\rho} (-\partial_\phi(B_z \rho \Omega)) \hat{z}. \end{aligned} \quad (21)$$

This can be further simplified with the use of the solenoidal condition  $\nabla \cdot \mathbf{B} = 0$  in cylindrical coordinates which is

$$\frac{1}{\rho} \frac{\partial(\rho B_\rho)}{\partial \rho} + \frac{1}{\rho} \frac{\partial B_\phi}{\partial \phi} + \frac{\partial B_z}{\partial z} = 0 \quad (22)$$

and we arrive at

$$\nabla \times (\mathbf{v} \times \mathbf{B}) = -\Omega \partial_\phi \mathbf{B} \quad (23)$$

where the partial derivative acts on the components of the vector only. Now, let

$$\mathbf{B} = \mathbf{B}_1 e^{im\phi} e^{-\lambda t} \quad (24)$$

where  $\mathbf{B}_1$  is a function of  $\rho$  and  $z$  only. Substituting all these terms into Eq. (15)

$$(\nabla^2 + k^2) \mathbf{B} = 0 \quad (25)$$

where

$$k^2 = \mu\sigma(\lambda - im\Omega). \quad (26)$$

If we wish a steady state field scenario is achieved if we set  $\lambda$  equal to zero. The problem is now reduced to solving the vector Helmholtz equation (Eq. (25)) which is not all that trivial.

For a transverse applied magnetic field we can safely assume no  $B_z$  component within the cylinder. Using the vector Laplacian the radial component of the Helmholtz equation is

$$\begin{aligned} (\nabla^2 \mathbf{B})_\rho &= \nabla^2 B_\rho - \frac{1}{\rho^2} B_\rho - \frac{2}{\rho^2} \frac{\partial B_\phi}{\partial \phi} \\ &= \frac{1}{\rho} \frac{\partial}{\partial \rho} \left( \rho \frac{\partial B_\rho}{\partial \rho} \right) + \frac{1}{\rho^2} \frac{\partial^2 B_\rho}{\partial \phi^2} - \frac{1}{\rho^2} B_\rho - \frac{2}{\rho^2} \frac{\partial B_\phi}{\partial \phi} \end{aligned} \quad (27)$$

after some manipulation and again using the solenoidal condition the Helmholtz equation for the  $\hat{\rho}$  component becomes

$$\rho^2 \frac{\partial^2 B_\rho^{in}}{\partial \rho^2} + 3\rho \frac{\partial B_\rho^{in}}{\partial \rho} + B_\rho^{in} + \frac{\partial^2 B_\rho^{in}}{\partial \phi^2} + \rho^2 k^2 B_\rho = 0 \quad (28)$$

Writing  $B_\rho$  component as  $B(\rho)e^{im\phi}$  and differentiating a Bessel equation is found:

$$\rho^2 \frac{d^2 B}{d\rho^2} + 3\rho \frac{dB}{d\rho} + (1 - m^2 - im\mu\sigma\Omega\rho^2)B = 0. \quad (29)$$

where we have set  $\lambda$  in Eq. (26) to zero so as to investigate the time independent case. (Bowman, 1958) gives the solution to the Bessel equation of the form

$$x^2 \frac{d^2 y}{dx^2} + (2p + 1)x \frac{dy}{dx} + (a^2 x^{2r} + \beta^2)y = 0 \quad (30)$$

as

$$y = x^{-p} \left[ C_1 J_{q/r} \left( \frac{a}{r} x^r \right) + C_2 Y_{q/r} \left( \frac{a}{r} x^r \right) \right], \quad (31)$$

where

$$q \equiv \sqrt{p^2 - \beta^2}. \quad (32)$$

Comparing Eq. (29) with Eq. (30) we pick out  $p = 1$  and  $r = 1$  and see that  $a^2 = -im\mu\sigma\Omega$  whilst  $\beta^2 = 1 - m^2$ . As such we see that  $q = m$ . Our general solution for  $B_\rho$  therefore consists of terms

$$B_\rho = \frac{1}{\rho} J_m(\sqrt{-im}\rho/\delta) e^{im\phi} \quad (33)$$

where we omit the Bessel functions of the second kind since we require the solution to be non-singular at  $\rho = 0$ . We can also omit all terms other than  $m = 1$ . The diffusion length  $\delta = (\mu\sigma\Omega)^{-1/2}$  has also been defined and it will be useful for later to define the magnetic Reynolds number  $R_m = (R/\delta)^2$  where  $R$  is the radius of the cylinder. Hence the solution inside the cylinder must be proportional to

$$B_\rho = \frac{1}{\rho} J_1(\sqrt{-im}\rho/\delta) e^{im\phi} \quad (34)$$

using Eq. (22) we can easily find the differential equation satisfied by  $B_\phi$

$$\frac{\partial B_\phi}{\partial \phi} = -\frac{\partial}{\partial \rho} (J_1(\sqrt{-im}\rho/\delta) e^{im\phi}). \quad (35)$$

Using the differentiation recurrence relation for Bessel functions of the first kind

$$\frac{\partial}{\partial z} J_\nu(z) = -\frac{\nu}{z} J_\nu(z) + J_{\nu-1}(z) \quad (36)$$

Eq. (35) becomes

$$\frac{\partial B_\phi}{\partial \phi} = \left( \frac{1}{\rho} J_1(\sqrt{-im}\rho/\delta) - \frac{\sqrt{-i}}{\delta} J_0(\sqrt{-im}\rho/\delta) \right) e^{im\phi} \quad (37)$$

The slightly tricky part of the procedure arises now: matching the internal and external fields.

Outside of the cylinder we need to solve the Laplace equation for the magnetic scalar potential  $\psi$ . The general solution with the correct azimuthal dependence is

$$\psi = (A\rho + B\rho^{-1})e^{im\phi}. \quad (38)$$

Where  $A$  and  $B$  are complex constants. Taking the gradient of  $\psi$  we result in

$$\mathbf{B}/\mu_o = -\nabla\psi = \hat{\rho} \left( A + \frac{B}{\rho^2} \right) e^{im\phi} + \hat{\phi} \left( A - \frac{B}{\rho^2} \right) ie^{im\phi} \quad (39)$$

where we have redefined  $A$  in going to the second equality. Now the boundary at the surface  $\rho = a$  are

$$B_\phi^{in}(a, \phi)/\mu = B_\phi^{ex}(a, \phi)/\mu_o \quad (40)$$

$$B_\rho^{in}(a, \phi) = B_\rho^{ex}(a, \phi). \quad (41)$$

Imposing these constraints and noticing that  $A$  can be identified with the magnetic field at infinity we can eliminate  $B$ .

We write down the full solution as:

$$B_{\rho}^{in} = Re \left\{ \frac{B_o(1 + R'^2/a^2)aJ_1(\rho\sqrt{-i}/\delta)e^{i\phi}}{\rho J_1(\sqrt{-iR_m})} \right\} \quad (42)$$

$$B_{\phi}^{in} = Re \left\{ \frac{iB_o(1 + R'^2/a^2)[\sqrt{-iR_m}J_0(\rho\sqrt{-i}/\delta) - (a/\rho)J_1(\rho\sqrt{-i}/\delta)e^{i\phi}]}{J_1(\sqrt{-iR_m})} \right\} \quad (43)$$

$$B_{\rho}^{ex} = Re \{ B_o(1 + R'^2/\rho^2)e^{i\phi} \} \quad (44)$$

$$B_{\phi}^{ex} = Re \{ iB_o(1 - R'^2/\rho^2)e^{i\phi} \}, \quad (45)$$

where  $R'$  is given by

$$R'^2 = a^2 \left[ \frac{(\mu/\mu_o + 1)J_1(\sqrt{iR_m}) - \sqrt{iR_m}J_0(\sqrt{iR_m})}{(\mu/\mu_o - 1)J_1(\sqrt{iR_m}) + \sqrt{iR_m}J_0(\sqrt{iR_m})} \right] \quad (46)$$

The lines of force are then plotted for various values of  $R_m$  in Figs. (3) to (6). It is clear that as we increase the magnetic Reynolds number the magnetic field gets completely shielded from the conducting cylinder and we are left purely with the constant external field and an induced dipole, entirely analogous to potential flow around a solid cylinder.

In this derivation, which follows (Perry and Jones, 1978), from the outset we have assumed the steady state condition  $\partial\mathbf{B}/\partial t = 0$ . This assumption vastly simplifies the analysis, however, we have missed some nice time dependent effects. (Parker, 1966) discusses extensively the instantaneous rotation of a sphere and cylinder in an initially uniform field. The analysis is rather involved and the time dependence in both the spherical and cylindrical case is factored in with the use of Laplace transforms, whose inversion via a contour integral results in an infinite sum of terms. A nice feature of the cylindrical case that we have not mentioned is that we can in fact contour a stream function  $V$  immediately. Notice that if we can write the magnetic field as

$$B_{\rho} = \frac{iV}{\rho} e^{i\phi}, \quad (47)$$

$$B_{\phi} = -\frac{\partial V}{\partial \rho} e^{i\phi}, \quad (48)$$

$$B_z = 0, \quad (49)$$

then both the solenoidal condition  $\nabla \cdot \mathbf{B} = 0$  as well as the streamline condition  $\mathbf{B} \cdot \nabla(Ve^{i\phi}) = 0$  are satisfied. The streamline condition immediately tells us that  $\mathbf{B}$  is perpendicular to the gradient of the function  $Ve^{i\phi}$  and hence parallel to contours of it. So the easiest way of representing the field inside the cylinder is to plot the

contours of this function.  $V$  is given by:

$$V = -\frac{2B_o a}{i^{1/2} R_m^{1/2}} \frac{J_1(i^{3/2} R_m^{1/2} r/a)}{J_0(i^{3/2} R_m^{1/2})} + \sum_{n=1}^{\infty} 4B_o a \frac{\exp(-i\Omega t - j_n^2 \Omega t / R_m) J_1(j_n r/a)}{j_n^2 (1 + j_n^2 / R_m) J_1(j_n)} \quad (50)$$

where  $j_n$  is the  $n$ th zero of the zeroth order Bessel function, that is:

$$J_0(j_n) = 0 \quad , \quad n = 1, 2, \dots, \infty. \quad (51)$$

Outside the cylinder we can find another field to contour. Starting with the magnetic scalar potential given in Eq. (38) enforcing the continuity of the radial component (Eq. 41) we arrive at the stream function outside of the cylinder:

$$U e^{i\phi} = (F(t)/\rho - B_o \rho) i e^{i\phi}, \quad (52)$$

where the dipole coefficient  $B$  in Eq. (38) has become time dependent and is now given by:

$$F(t) = -iRV(R) + B_o R^2, \quad (53)$$

where  $V(R)$  is Eq. (50) evaluated at  $\rho = R$ .

### 3. Rotating Sphere in a Transverse Field

It is now natural to work in spherical coordinates. Using Eq. (15) and writing the velocity  $\mathbf{v} = \Omega r \sin \theta \hat{\theta}$  and the field as  $\mathbf{B} = B_r \hat{r} + B_{\theta} \hat{\theta} + B_{\phi} \hat{\phi}$  the  $\mathbf{v} \times \mathbf{B}$  term evaluates to  $B_r \Omega r \sin \theta \hat{\theta} - B_{\theta} \Omega r \sin \theta \hat{r}$ . We now take the curl in spherical polar coordinates

$$\begin{aligned} \nabla \times (B_r \Omega r \sin \theta \hat{\theta} - B_{\theta} \Omega r \sin \theta \hat{r}) &= \\ \frac{1}{r \sin \theta} (-\partial_{\phi}(B_r \Omega r \sin \theta)) \hat{r} + \\ \frac{1}{r} \left( \frac{1}{\sin \theta} \partial_{\phi}(-B_{\theta} \Omega r \sin \theta) \right) \hat{\theta} + \\ \frac{1}{r} (\partial_r(rB_r \Omega r \sin \theta) - \partial_{\theta}(B_{\theta} \Omega r \sin \theta)) \hat{\phi}. \end{aligned} \quad (54)$$

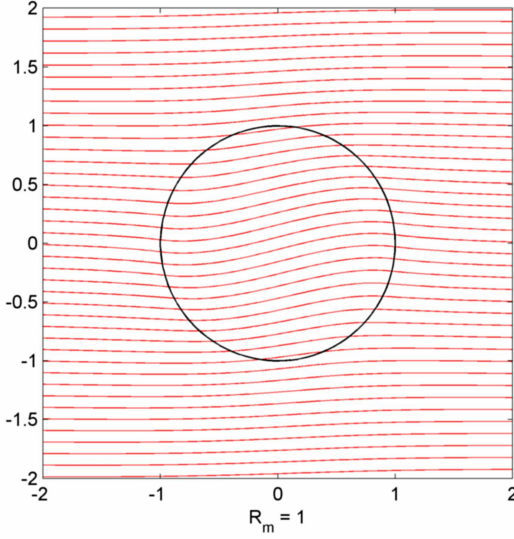


FIG. 3

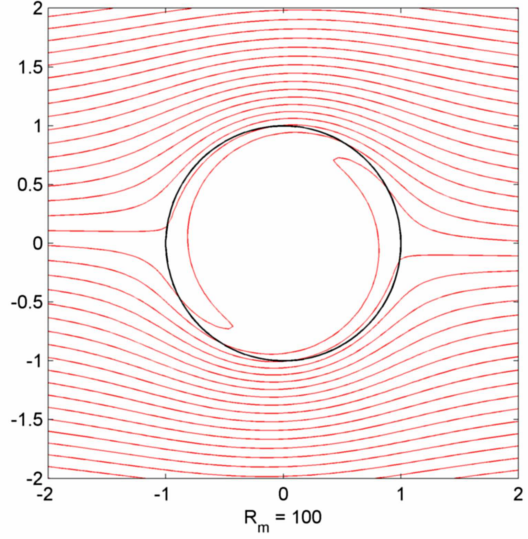


FIG. 5

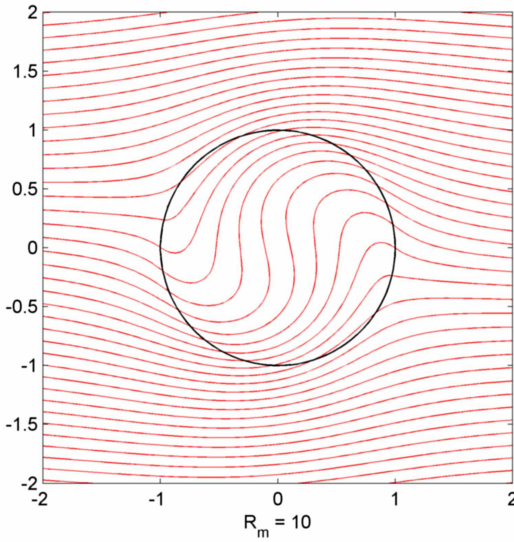


FIG. 4

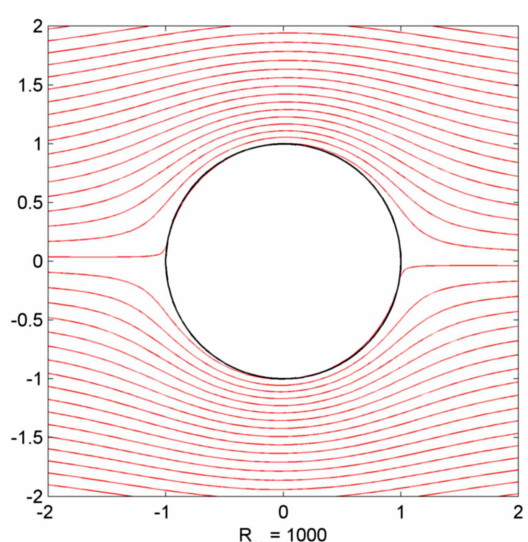


FIG. 6

The first two terms clearly simplify to  $-\Omega\partial_\phi B_r \hat{\mathbf{r}}$  and  $-\Omega\partial_\phi B_\theta \hat{\boldsymbol{\theta}}$  respectively. The third term requires a little more work and we have to use the fact that  $\nabla \cdot \mathbf{B} = 0$  in spherical coordinates means:

$$\frac{1}{r^2} \partial_r(r^2 B_r) + \frac{1}{\sin \theta} \partial_\theta(B_\theta \sin \theta) = -\frac{1}{\sin \theta} \partial_\phi B_\phi. \quad (55)$$

Hence we can write the full equation as

$$-\nabla^2 \mathbf{B}/\mu\sigma = -\frac{\partial \mathbf{B}}{\partial t} - \Omega\partial_\phi \mathbf{B}. \quad (56)$$

where the partial derivative with respect to  $\phi$  acts only on the field components and not on the basis vectors.

Once again we have arrived at the vector Helmholtz equation, but this time it will be necessary to work in spherical coordinates.

Once again we can discuss the time dependent case whereby the solid conducting sphere is set spinning at  $\Omega$  instantaneously in a uniform external field. The derivation again is to be found in (Parker, 1966). Unfortunately in the spherical case there is no analogous stream function to Eq. (50) and instead we have to proceed by calculating components and integrating the field line equations numerically. For completeness we write down the scalar field  $S$  from which the internal vector field can be

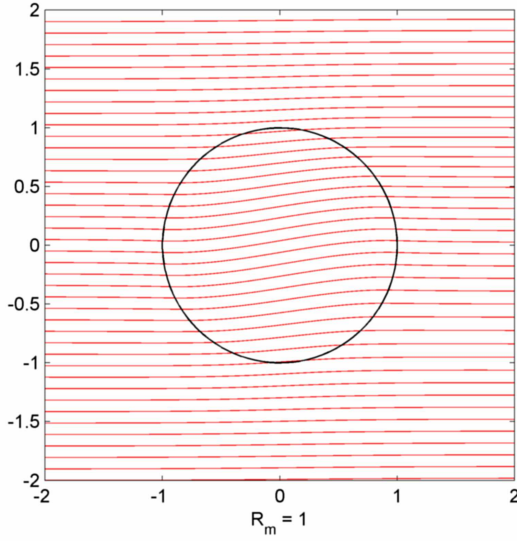


FIG. 7

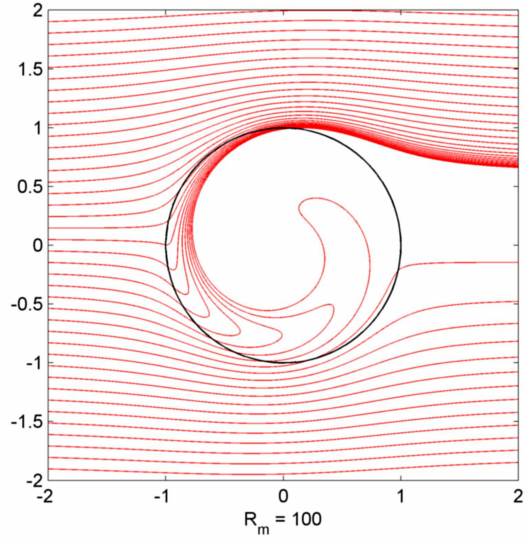


FIG. 9

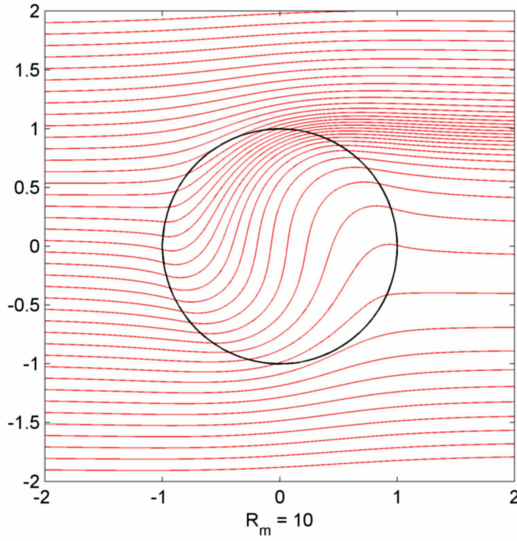


FIG. 8

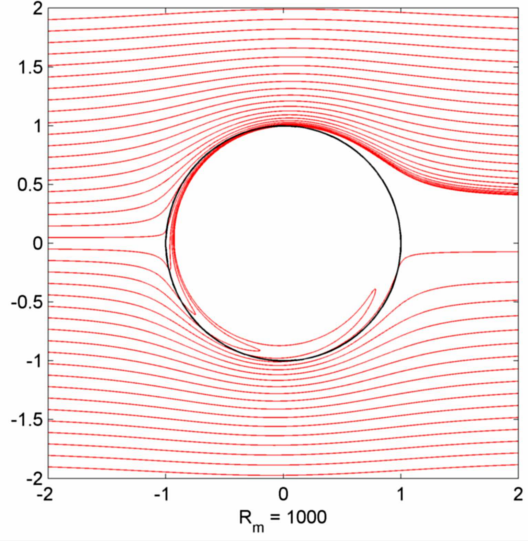


FIG. 10

derived:

$$S = \frac{3}{2} \frac{B_o (a^3 r)^{1/2}}{i^{3/2} R_m^{1/2}} \frac{J_{3/2}(i^{3/2} R_m^{1/2} r/a)}{J_{1/2}(i^{3/2} R_m^{1/2})} + \sum_{n=1}^{\infty} 3 B_o i (a^3 r)^{1/2} \frac{\exp(-i\Omega t - n^2 \Omega t / R_m) J_{3/2}(n\pi r/a)}{n^2 \pi^2 (i + n^2 \pi^2 / R_m) J_{3/2}(n\pi)}. \quad (57)$$

The magnetic field components are then given by:

$$B_r = \frac{2}{r^2} \sin \theta e^{i\phi}, \quad (58)$$

$$B_\phi = \frac{\partial S}{\partial r} \cos \theta e^{i\phi}, \quad (59)$$

$$B_\theta = \frac{1}{r \sin \theta} \frac{\partial S}{\partial r} \sin \theta e^{i\phi}. \quad (60)$$

For completeness:

$$\begin{aligned} \frac{\partial S}{\partial r} = & \frac{3}{2} \frac{B_o a^{3/2}}{i^{3/2} R_m^{1/2} J_{1/2}(i^{3/2} R_m^{1/2})} \left[ \frac{i^{3/2} R_m^{1/2} r}{a} J_{1/2}(i^{3/2} R_m^{1/2} r/a) - J_{3/2}(i^{3/2} R_m^{1/2} r/a) \right] \\ & + \sum_{n=1}^{\infty} \frac{3B_o ia^{3/2} \exp(-i\Omega t - n^2 \Omega t / R_m) J_{3/2}(n\pi r/a)}{r^{1/2} n^2 \pi^2 (i + n^2 \pi^2 / R_m) J_{3/2}(n\pi)} \left[ \frac{n\pi}{a} J_{1/2}(n\pi r/a) - J_{3/2}(n\pi r/a) \right]. \end{aligned} \quad (61)$$

Once again we match the external field, which is a combination of a constant uniform field and a time dependent dipole field. In spherical coordinates the dipole field is

$$B_r = (B_o - 2 \frac{F(t)}{r^2}) \sin \theta e^{i\phi}, \quad (62)$$

$$B_\phi = (B_o + \frac{F(t)}{r^2}) \cos \theta e^{i\phi}, \quad (63)$$

$$B_\theta = \frac{1}{\sin \theta} (B_o + \frac{F(t)}{r^2}) i e^{i\phi}. \quad (64)$$

From the continuity equations we now find that

$$F(t) = \frac{1}{2} B_o a^2 - S(a). \quad (65)$$

It is worth comparing the stationary fields of the rotating cylinder and sphere as shown in Fig. (3-10). They share a notable number of similarities as one would expect. However, the voids of field lines to the right hand sides of the rotating spheres looks alarming, but there is nothing to worry about. Indeed this is just a remnant of the way the figures were created. On the one hand, for the cylinder it was analytically possible to uniformly contour a function and hence we result in nice, reasonably symmetrical diagrams. With the sphere on the other hand, the stream lines had to be calculated with brute force with a numerical integrator which steps along the field line and which were crucially seeded at some initial set of values. Doing so will invariably not reflect the behaviour of the field at the opposing side of the diagram. From the boundary conditions at infinity we know the fields must approach a uniform one. Perhaps it would be better to then seed the field from both sides. To try not to confuse matters we have seeded in blue from the right and in red from the left.

This somewhat helps resolve the issue, at the expense of some unevenly spaced field lines. But since field lines have no real physical interpretation we can leave it there and be happy with it.

### III. ELECTRIC FIELD LINES

We now move on to some examples of electric field lines. There are many great similarities between electric and magnetic field lines, which one would expect from Maxwell's equations.

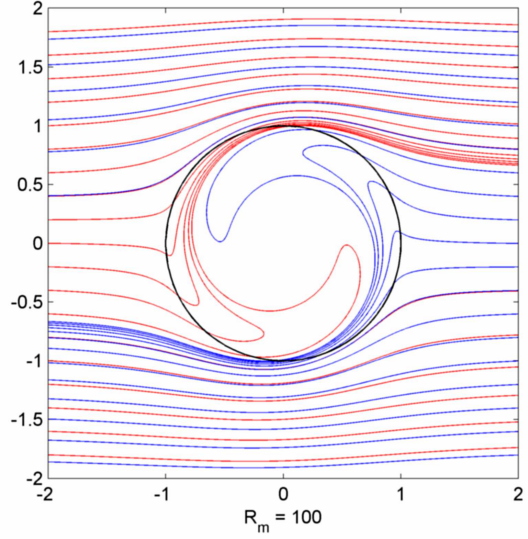


FIG. 11

#### A. Method of images

##### 1. Point charges and planes

The method of images is a way to solve Poisson's equation. The simplest application of the method of images is that of point charges interacting with planar geometries. A more interesting example of this type is that of a point charge between two grounded conducting plates. This case in fact involves an infinite number of image charges. Of course in the program we truncate the summation at a finite value. The potential is rather easy to write down, although the derivations of it can vary in length (Kellogg, 1929). For a unit charge situated at  $x = c$  between two grounded parallel conducting plates at  $x = 0$  and  $x = a$  we have:

$$V(x, z) = \sum_{n=-\infty}^{\infty} \left[ \frac{1}{\sqrt{(x - 2na - c)^2 + z^2}} - \frac{1}{\sqrt{(x - 2na + c)^2 + z^2}} \right]. \quad (66)$$

Using Eq. (66) it is a simple procedure to produce the fields

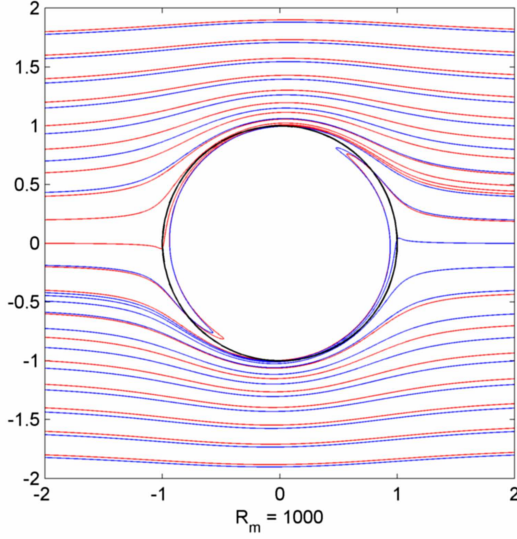


FIG. 12 Seeding uniformly from both sides.

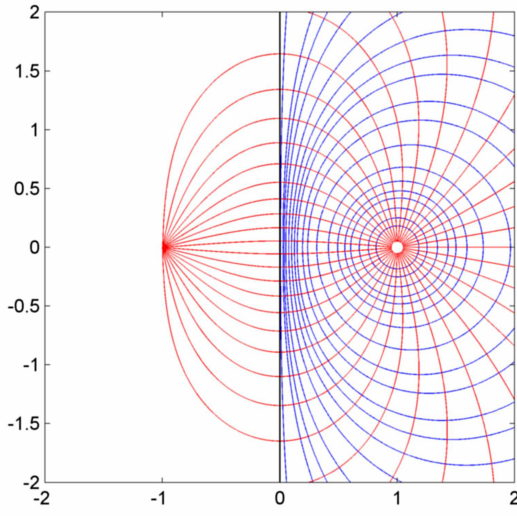


FIG. 13 Electric potential and field lines for a point charge situated in the region  $z > 0$  and a grounded conducting plane at  $z = 0$ . The field lines are seeded from the physical charge.

When we zoom in it is even more clear that the boundary conditions are satisfied

Po

## 2. The point charge and conducting sphere

A clever use of the method of images is the case of a point charge in the presence of a grounded conducting sphere. The boundary condition for the system is that the potential  $V(\mathbf{r})$  vanishes on the surface of the

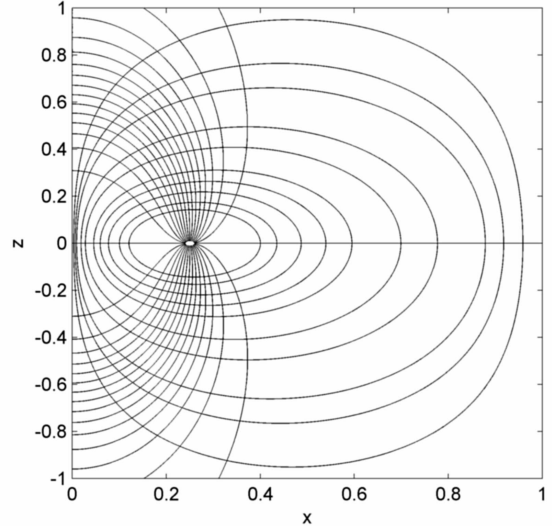


FIG. 14 A point charge situated at  $c = a/4$ . The grounded plates lie at  $x = 0$  and  $x = 1$ .

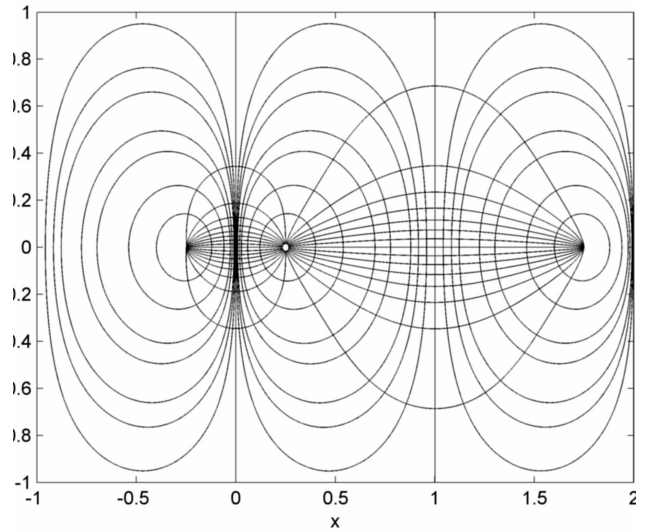


FIG. 15 The point charge remains at  $c = a/4$  but now we can see the action of two of the infinite number of required image charges. The first two are of opposite sign and we can see we have an arrangement akin to two dipoles.

grounded sphere, that is  $V(|\mathbf{r}| = a) = 0$ . If the physical charge  $q$  is placed a distance  $b$  from the centre of the sphere then the appropriate boundary conditions can be fulfilled if we place an image charge  $q'$  at  $z' = a^2/b$  and of magnitude  $q' = -(a/b)q$  along the line connecting the physical charge  $q$  and the centre of the sphere. These fields are shown in Fig. (??).

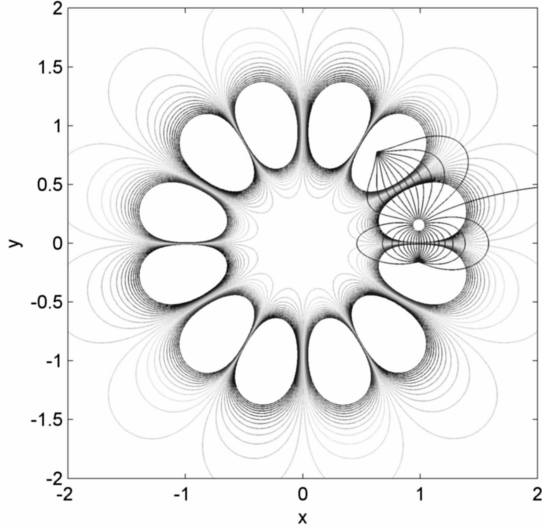


FIG. 16 In the special case where two conducting wedges are an integer submultiple of  $\pi$  we can solve the problem with a finite number of image points.

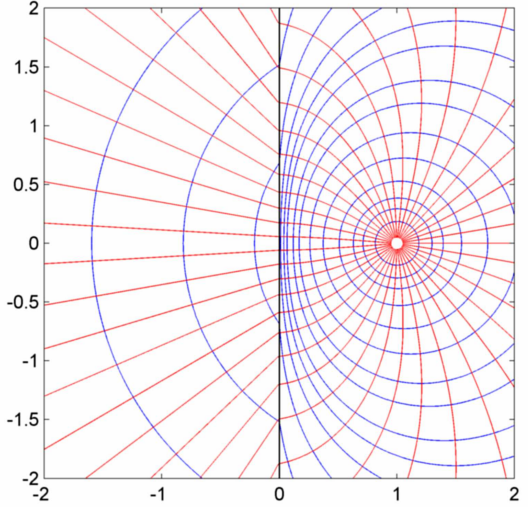


FIG. 18 Electric potential and field lines for a point charge situated in the region  $z > 0$  with  $\epsilon_1$  while for  $z < 0$  the relative permittivity is  $\epsilon_2$  and  $\epsilon_1 < \epsilon_2$ . Exact values are  $\epsilon_1 = 1$  and  $\epsilon_2 = 10$ .

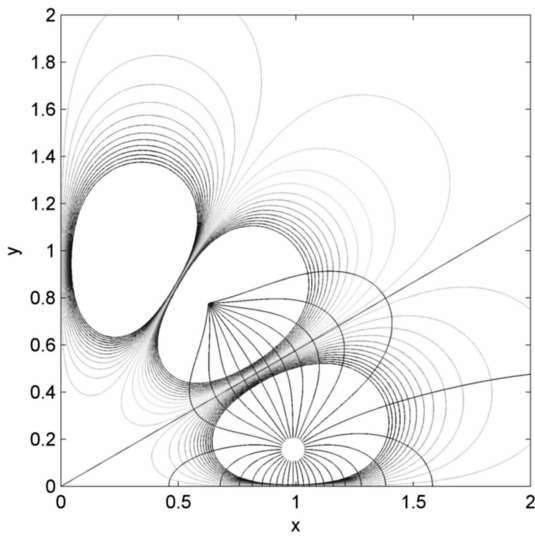


FIG. 17 Zoomed in version of Fig. (16)

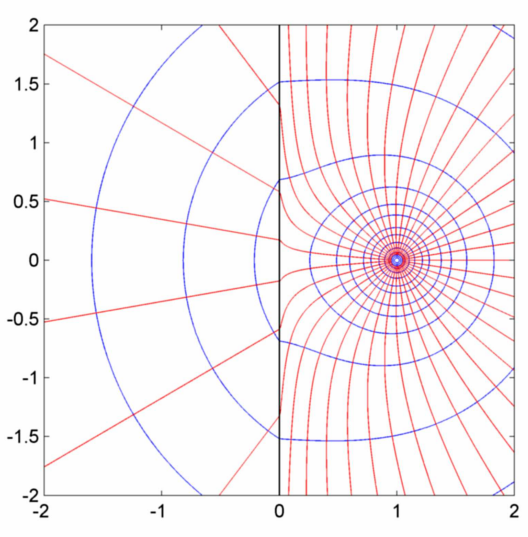


FIG. 19 The opposite case:  $\epsilon_1 > \epsilon_2$ .  $\epsilon_1 = 10$  and  $\epsilon_2 = 1$ .

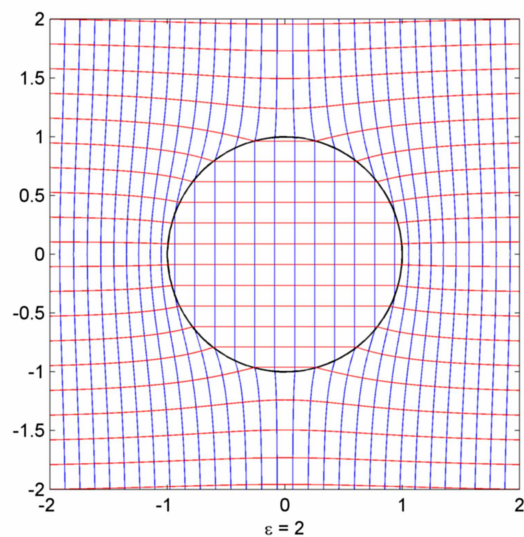


FIG. 20

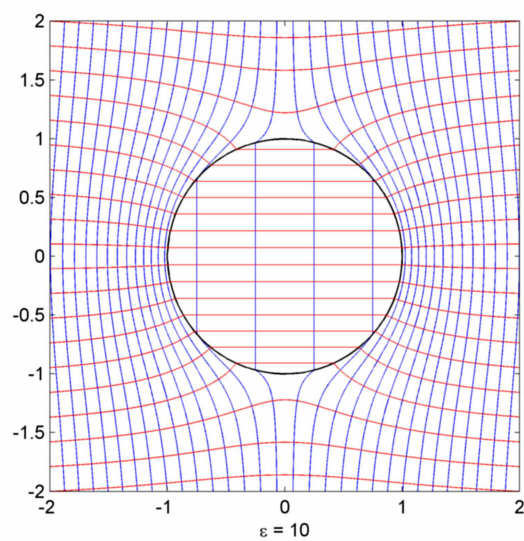


FIG. 21

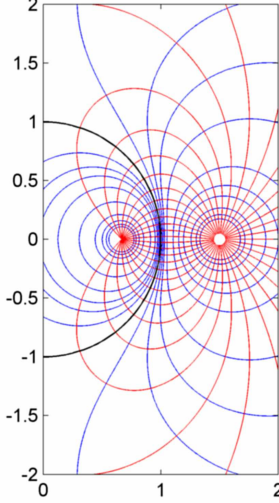


FIG. 22 Electric potential and field lines for a point charge outside a conducting sphere with the presence of the image charge. It has to be noted that the electric field vanishes within the conductor and of course the potential is constant and zero throughout the whole sphere. The field lines are included to show the presence of the image charge.

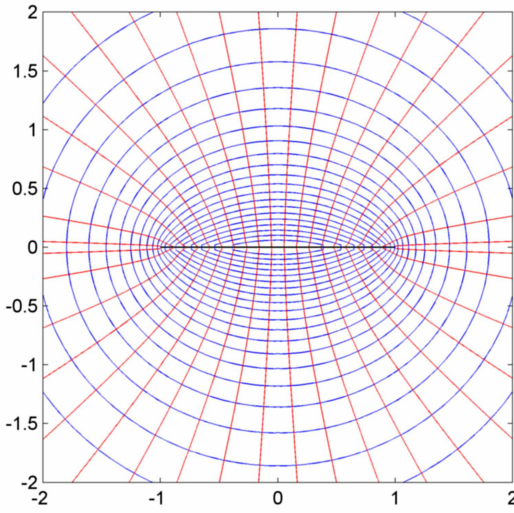


FIG. 23 The equipotentials and field lines of a uniformly charged disc.

### B. The uniformly charged disc

The uniformly charged disc provides an interesting and useful example.

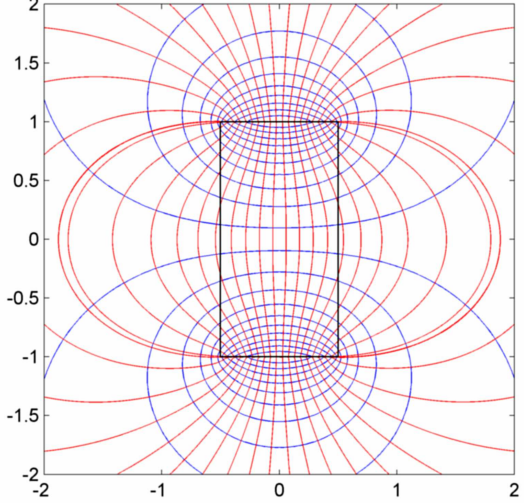


FIG. 24 Two oppositely charged discs have an identical form of the fields of a cylindrical bar magnet.

### 1. Point charge outside a dielectric sphere

It is impossible to use image charges in the case of a dielectric sphere. Instead an azimuthally symmetric solution of the Poisson equation is needed. The fields for the point charge outside a dielectric sphere are given by (Cai, Deng, and Jacobs, 2007):

$$V(r, \theta) = \begin{cases} \sum_{n=0}^{\infty} C_n r^n P_n(\cos \theta), & 0 \leq r \leq a, \\ \sum_{n=0}^{\infty} \left[ \frac{q}{4\pi\epsilon_0 b} \left( \frac{r}{b} \right)^n + \frac{D_n}{r^{n+1}} \right] P_n(\cos \theta), & a \leq r \leq b, \\ \sum_{n=0}^{\infty} \left[ \frac{q}{4\pi\epsilon_0 r} \left( \frac{b}{r} \right)^n + \frac{D_n}{r^{n+1}} \right] P_n(\cos \theta), & b \leq r, \end{cases} \quad (67)$$

where  $C_n$  and  $D_n$  in Eq.(67) are given by

$$C_n = \frac{q}{4\pi\epsilon_0} \frac{1}{b^{n+1}} \frac{1-\gamma}{2} \left( 2 + \frac{2\gamma}{1-\gamma+2n} \right), \quad (68)$$

$$D_n = -\frac{q}{4\pi\epsilon_0} \frac{a^{2n+1}}{b^{n+1}} \gamma \left( 1 - \frac{1-\gamma}{1-\gamma+2n} \right). \quad (69)$$

and  $\gamma = (\epsilon_i - \epsilon_o) / (\epsilon_i + \epsilon_o)$ .

### C. Complex potentials

It is well known that the theory of complex variables can be applied to electrostatics. The key result is that any analytic function  $f = u + iv$  of a complex variable  $z = x + iy$  gives two real functions  $u(x, y)$  and  $v(x, y)$  which are possible electric potential functions.

A very nice result is achieved with the use of

$$z = f + e^f. \quad (70)$$

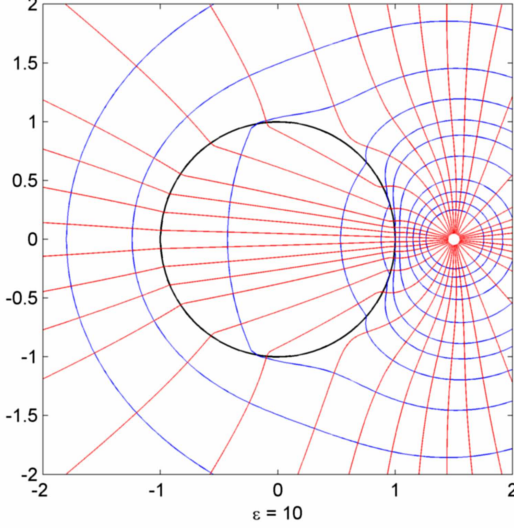


FIG. 25 Electric potential and field lines for a point charge outside a dielectric sphere

This equation cannot be inverted to the form  $f(z)$ ; however, when we write  $z = x + iy$  and  $f = u + iv$  and equate real and imaginary parts of Eq.(70) we arrive at

$$x = u + e^u \cos v \quad (71)$$

$$y = v + e^u \sin v. \quad (72)$$

Equipotentials can then be taken as surfaces of constant  $v = V$  and the equations of these lines are then written in terms of the parameter  $u$ . That is, the equipotentials are given by

$$x = u + e^u \cos V, \quad y = V + e^u \sin V, \quad (73)$$

where  $-\pi \leq V \leq \pi$  fills the complex plane with curves. A similar procedure can then be applied for the field lines by plotting curves of constant  $u$  and varying  $v$ . We then arrive at Fig.(26) which can indeed be found in Maxwell's Treatise (Maxwell, 1873).

#### D. Electric dipole radiation

The exact solution of for the  $\mathbf{E}$  field of an electric dipole  $\mathbf{P} = \mathbf{p}e^{-i\omega t}$  is given by

$$\mathbf{E} = \frac{1}{4\pi\epsilon_0} \left\{ k^2 (\hat{\mathbf{n}} \times \mathbf{p}) \times \hat{\mathbf{n}} \frac{e^{i(kr-\omega t)}}{r} + [3\hat{\mathbf{n}}(\hat{\mathbf{n}} \cdot \mathbf{p}) - \mathbf{p}] \left( \frac{1}{r^3} - \frac{ik}{r^2} \right) e^{i(kr-\omega t)} \right\} \quad (74)$$

and the  $\mathbf{B}$  field is given by

$$\mathbf{B} = \frac{\mu_0 c}{4\pi} k^2 p (\hat{\mathbf{n}} \times \mathbf{p}) \left( \frac{1}{r} - \frac{1}{ikr^2} \right) e^{i(kr-\omega t)} \quad (75)$$

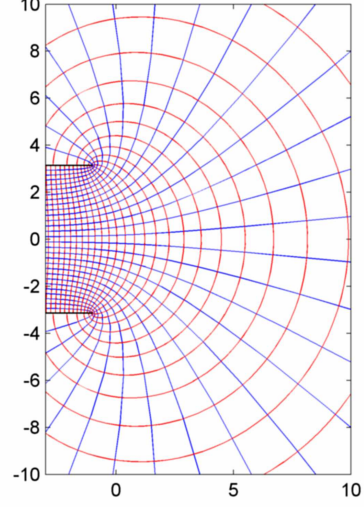
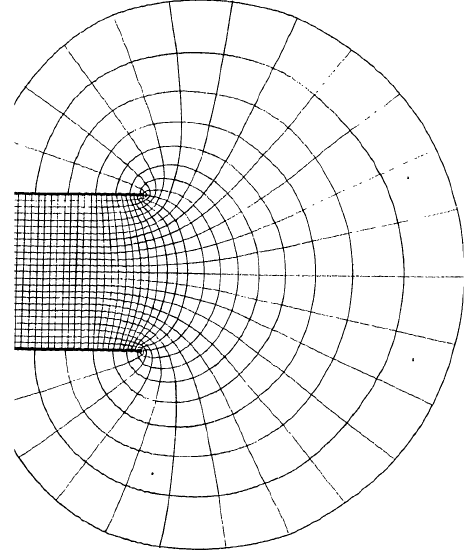


FIG. 26 Capacitor field lines



*Lines of Force between two Plates.*

FIG. 27 The remarkable field lines of a capacitor as drawn by Maxwell.

where  $p = \mathbf{p}/|\mathbf{p}|$ . With some effort it is then possible to write Eq. (74) in the form

$$\mathbf{E} = \frac{1}{4\pi\epsilon_0} \nabla \times \left\{ \left[ \frac{\mathbf{p}e^{i(kr-\omega t)}}{r^2} - \frac{i\omega \mathbf{p}e^{i(kr-\omega t)}}{cr} \right] \times \hat{\mathbf{n}} \right\} \quad (76)$$

and as such we have written the field as the curl of another vector field. Like in II.A we can simply contour  $\rho$  with the azimuthal component of this vector to get the field lines, saving a lot of work.

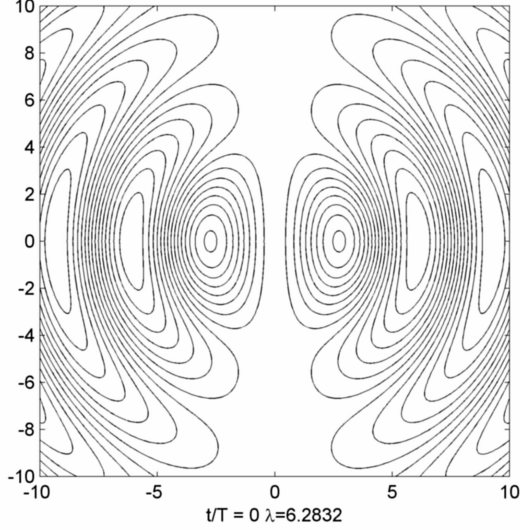


FIG. 28

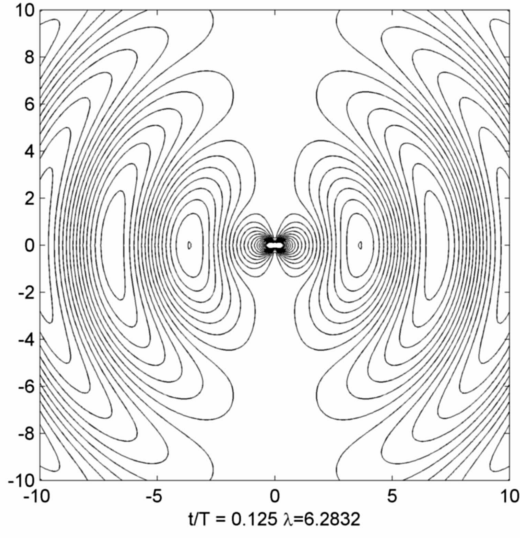


FIG. 29

### E. Relativistic field lines

It is natural to generalise field lines to those case in which sources are moving at relativistic speeds.

$$\mathbf{E} = \frac{q}{4\pi\epsilon_0} \left( \frac{1-\beta^2}{R^2} \frac{((\hat{\mathbf{n}} - \boldsymbol{\beta}))}{(1 - \hat{\mathbf{n}} \cdot \boldsymbol{\beta})^2} + \frac{\hat{\mathbf{n}} \times ((\hat{\mathbf{n}} - \boldsymbol{\beta}) \times \dot{\boldsymbol{\beta}})}{R(1 - \hat{\mathbf{n}} \cdot \boldsymbol{\beta})^2} \right) \quad (77)$$

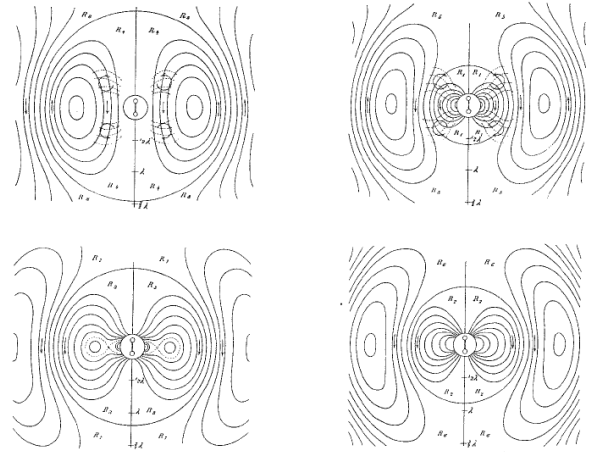


FIG. 30 Drawings of the field lines of a dipole by Hertz.

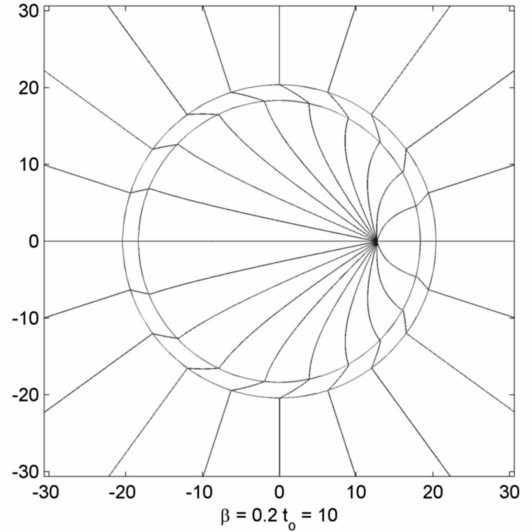


FIG. 31

1. Uniformly accelerated charge
2. Uniform circular motion
3. Harmonically oscillating charge

### IV. NUMERICAL WORK

The previous examples are all cases of nice enough analytical solutions. Of course in general

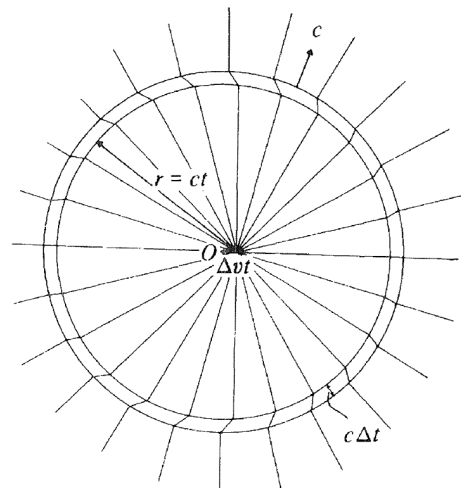


FIG. 32

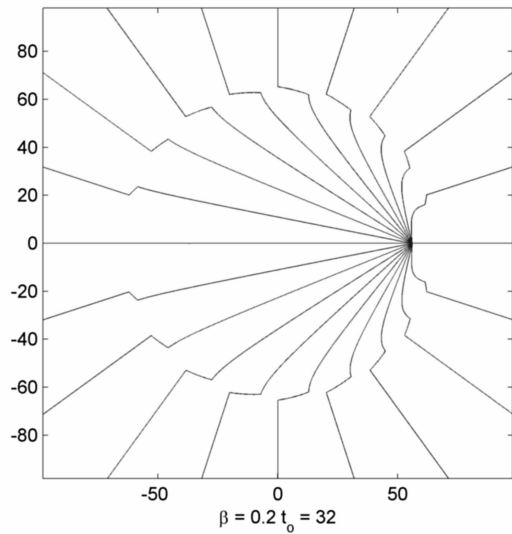


FIG. 33

**A. Finite difference methods****B. Solving the field line equations**

1. Runge-Kutta methods

The go to method for solving the differential equations.

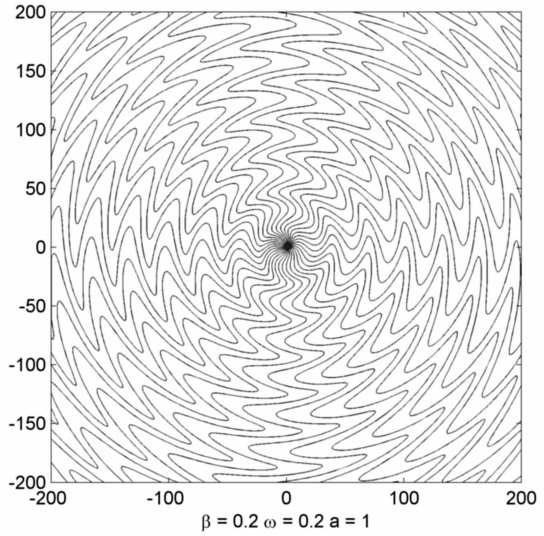


FIG. 34

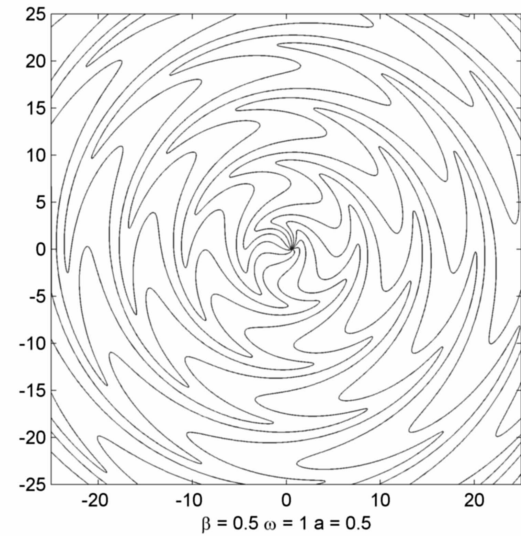


FIG. 35

**Appendix A: First Appendix**

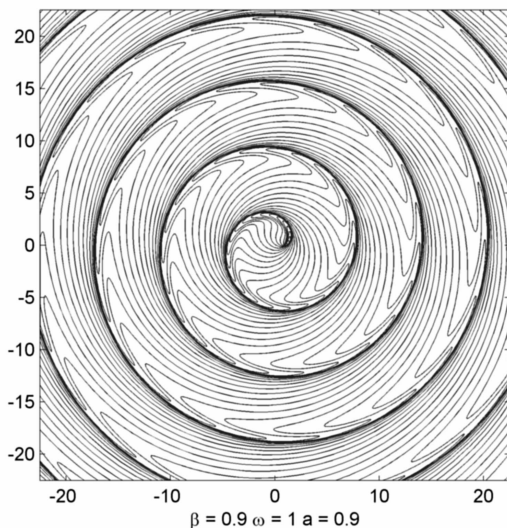


FIG. 36 Highly relativistic field lines of synchrotron radiation

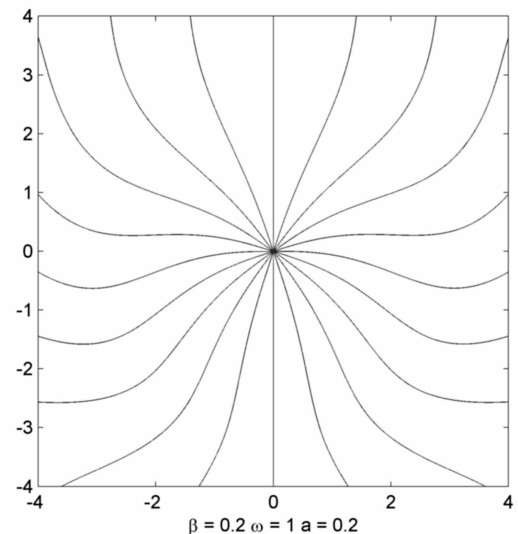


FIG. 38 Mildly relativistic field lines of dipole radiation

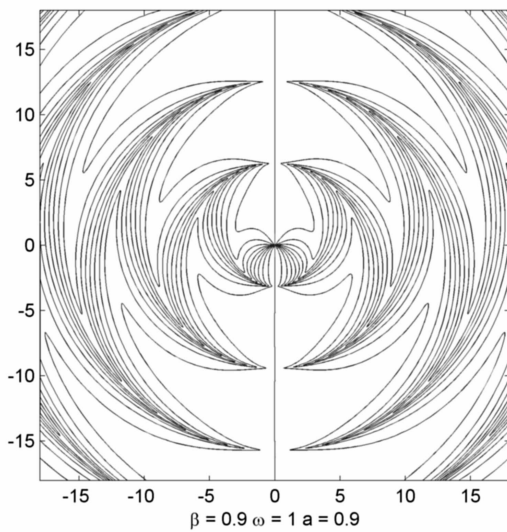


FIG. 37 Highly relativistic field lines of dipole radiation

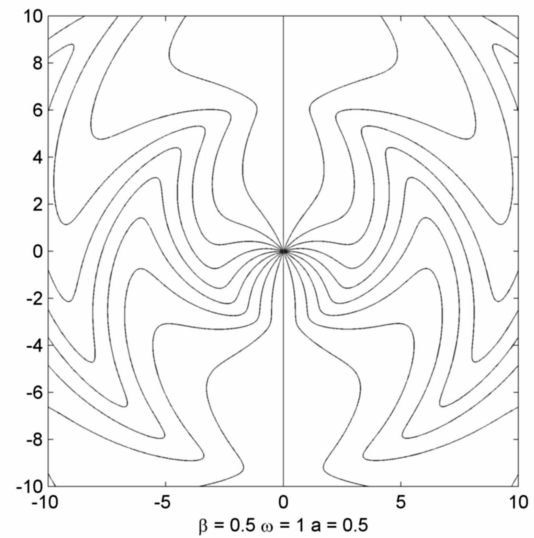
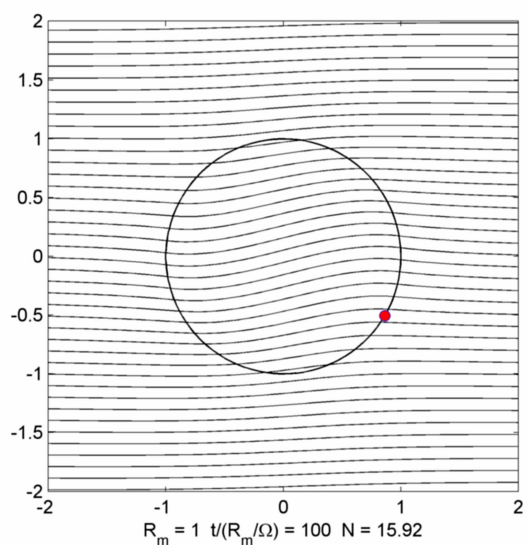
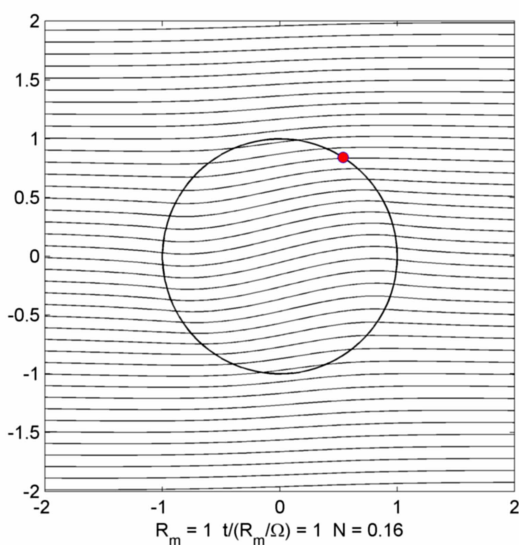
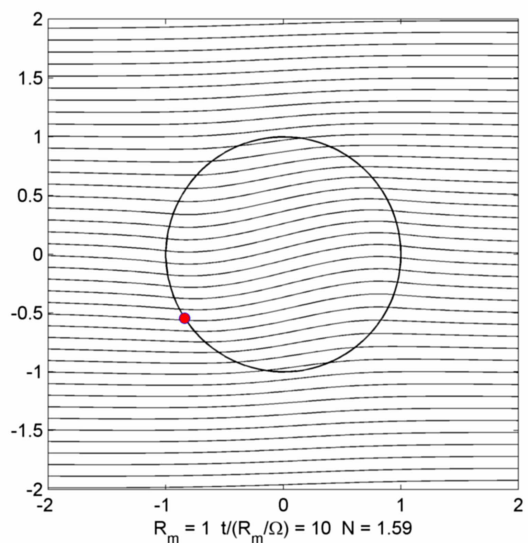
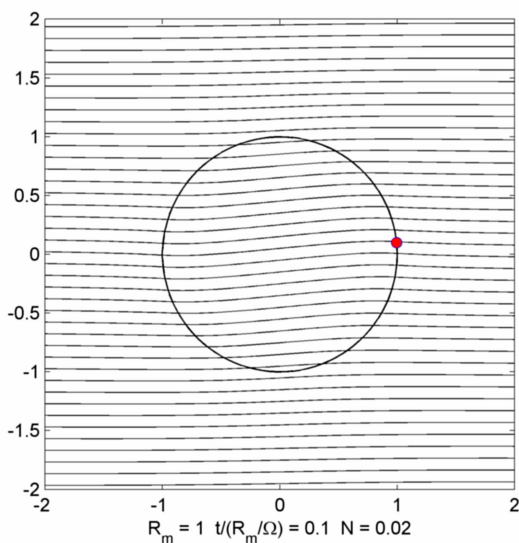


FIG. 39 Mildly relativistic field lines of dipole radiation



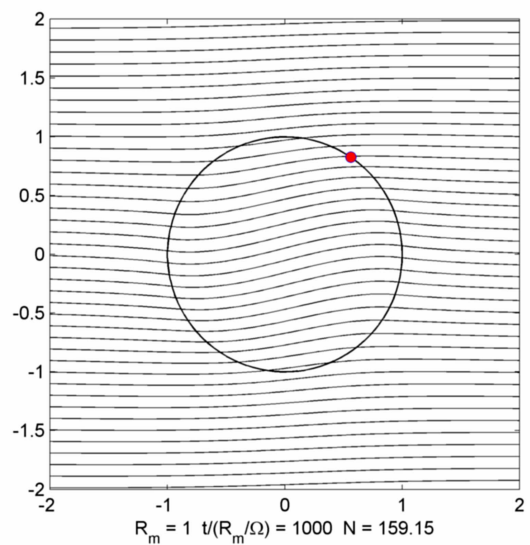


FIG. 44

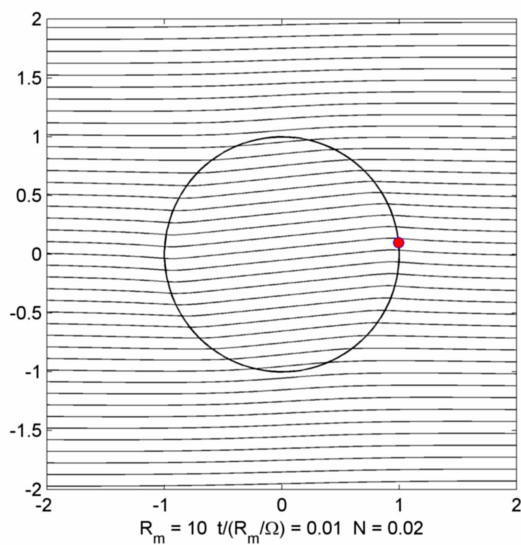


FIG. 45

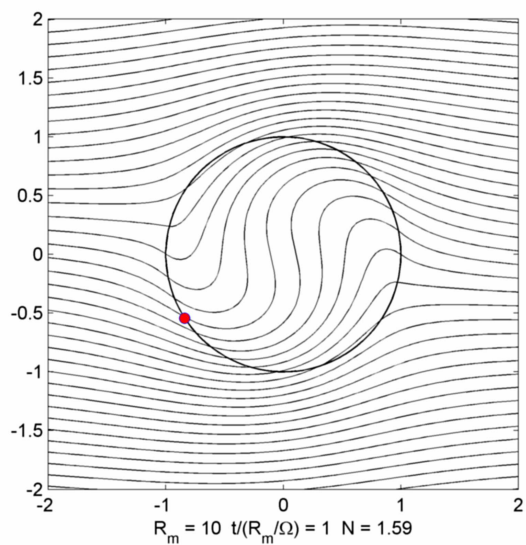


FIG. 47

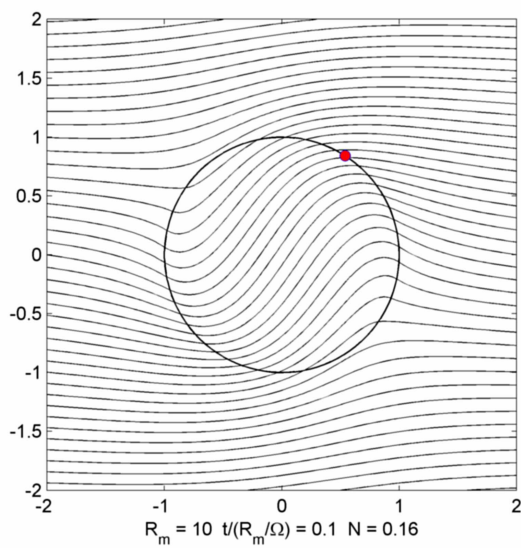


FIG. 46

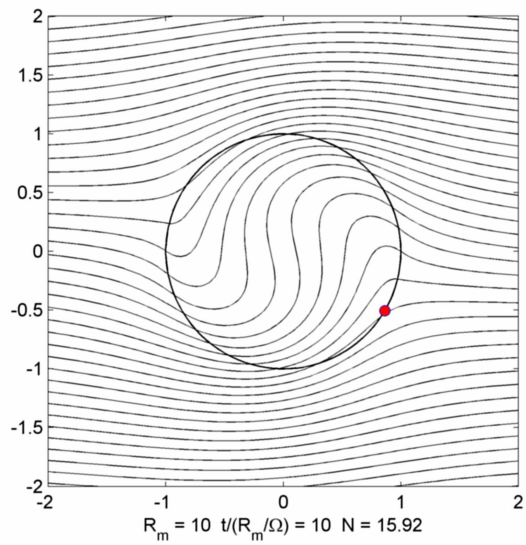


FIG. 48

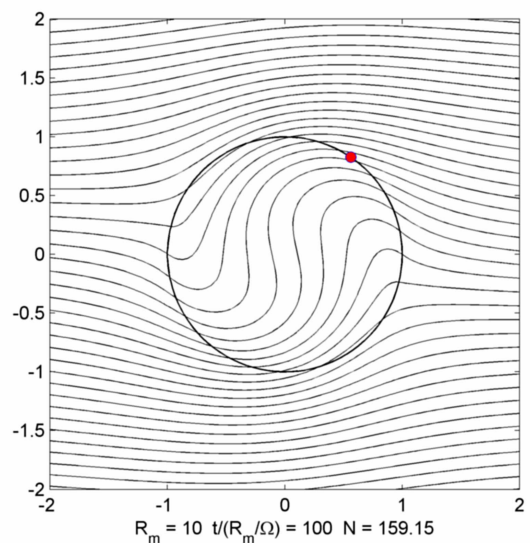


FIG. 49

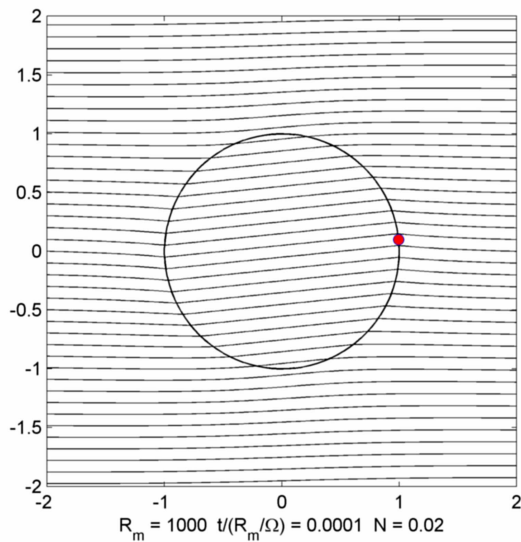


FIG. 50

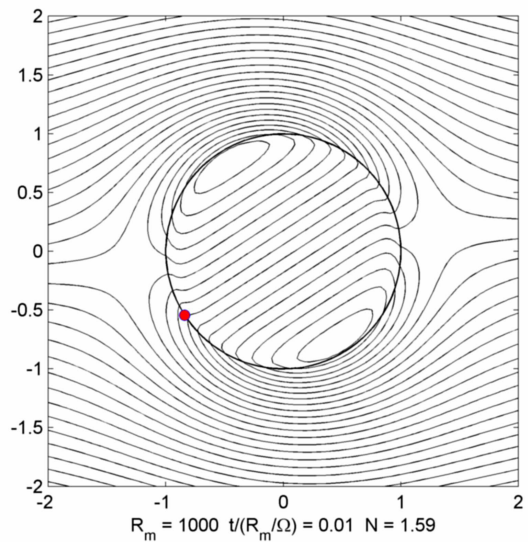


FIG. 52

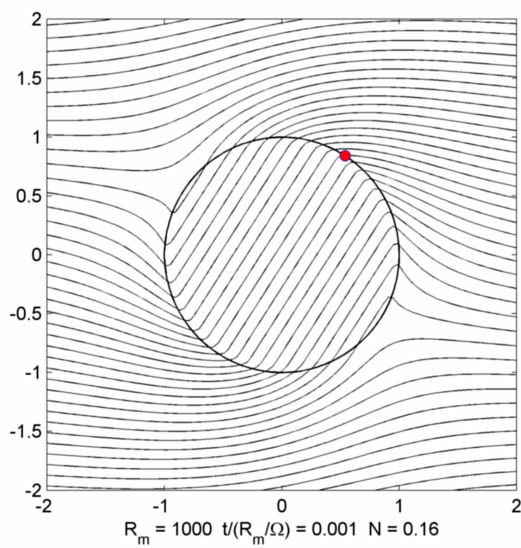


FIG. 51

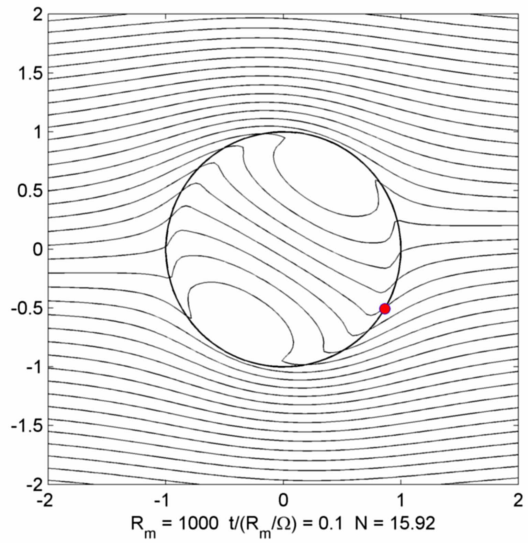


FIG. 53

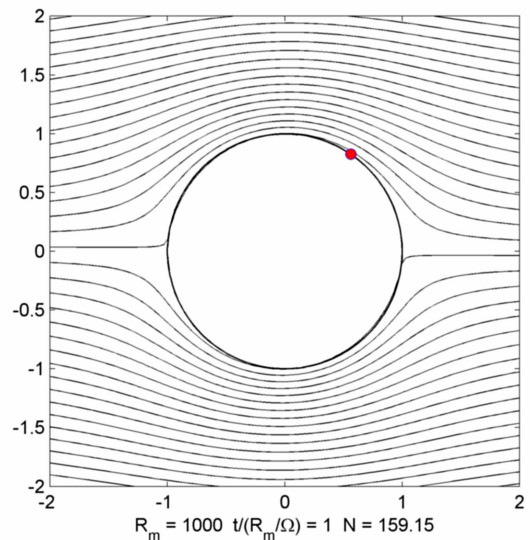


FIG. 54

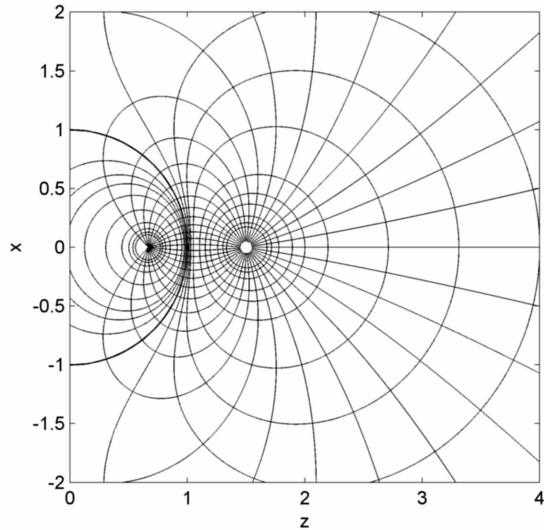


FIG. 55 Electric potential and field lines for a point charge outside a grounded conducting sphere-half view

## REFERENCES

- Bowman, F., *Introduction to Bessel functions* (Courier Corporation, 1958).
- Cai, W., Deng, S., and Jacobs, D., *Journal of Computational Physics* **223**, 846 (2007).
- Jackson, J. D., *Classical Electrodynamics*, 3rd Edition, by John David Jackson, pp. 832. ISBN 0-471-30932-X. Wiley-VCH, July 1998. **1** (1998).
- Kellogg, O. D., (1929).
- Maxwell, J., *Transactions of the Cambridge Philosophical Society* **10**, 27 (1864).
- Maxwell, J. C., *The London, Edinburgh, and Dublin Philosophical Magazine and Journal of Science* **21**, 161 (1861).
- Maxwell, J. C., (1873).
- Parker, R. L., *Proceedings of the Royal Society of London A: Mathematical, Physical and Engineering Sciences* **291**, 60 (1966).
- Perry, M. P. and Jones, T., *Magnetics, IEEE Transactions on* **14**, 227 (1978).